

Cite this: *J. Mater. Chem. A*, 2015, 3, 11527Received 6th March 2015  
Accepted 13th April 2015

DOI: 10.1039/c5ta01719j

www.rsc.org/MaterialsA

## Ultra-low thermal conductivity in TiO<sub>2</sub>:C superlattices

Janne-Petteri Niemelä,<sup>a</sup> Ashutosh Giri,<sup>b</sup> Patrick E. Hopkins<sup>b</sup> and Maarit Karppinen<sup>\*a</sup>

TiO<sub>2</sub>:C superlattices are fabricated from atomic/molecular layer deposited (ALD/MLD) inorganic–organic [(TiO<sub>2</sub>)<sub>m</sub>(Ti–O–C<sub>6</sub>H<sub>4</sub>–O)<sub>k=1</sub>]<sub>n</sub> thin films *via* a post-deposition annealing treatment that converts the as-deposited monomolecular organic layers into sub-nanometer-thick graphitic interface layers confined within the TiO<sub>2</sub> matrix. The internal graphitic layers act as effective phonon-scattering boundaries that bring about a ten-fold reduction in the thermal conductivity of the films with a decreasing superlattice period down to an ultra-low value of  $0.66 \pm 0.04 \text{ W m}^{-1} \text{ K}^{-1}$  – a finding that makes inorganic–C superlattices fabricated by the present method promising structures for *e.g.* high-temperature thermal barriers and thermoelectric applications.

## Introduction

Materials with ultra-low thermal conductivity are needed, *e.g.*, for thermal-barrier and thermoelectric applications; the latter application calls for novel heavily doped semiconductors able to combine thermal insulation with high electronic conductivity and thermopower. General pathways to suppress thermal transport in fully dense solid materials exploit the introduction of structural disorder in the form of, *e.g.*, point defects, alloying components, amorphous phases, grain boundaries or material interfaces. Both experiments and theory have shown that the introduction of material interfaces is particularly well harnessed in various superlattice and multilayer thin-film materials where the interfaces between alternating layers of dissimilar materials act as phonon-scattering boundaries: not only may thermal conductivity be suppressed by an order of magnitude across the film plane<sup>1,2</sup> but a significant drop may also be seen in the in-plane direction.<sup>3,4</sup> Furthermore, careful balancing between order and disorder in multilayers may enable achieving ultra-low thermal conductivities comparable to or even lower than those of amorphous or porous materials, as evidenced by the results for, *e.g.*, W/Al<sub>2</sub>O<sub>3</sub> nanolaminates ( $\sim 0.6 \text{ W m}^{-1} \text{ K}^{-1}$ ) and layered WSe<sub>2</sub> crystals ( $\sim 0.05 \text{ W m}^{-1} \text{ K}^{-1}$ ).<sup>5–7</sup>

For small-period superlattices, the dominance of the phonon-boundary scattering at the internal interfaces over the scattering by the bulk of the constituent materials enables the control of thermal conductivity through careful adjustment of the superlattice period;<sup>8</sup> efficient suppression is achieved for incoherent phonons by decreasing the period, until potentially,

phonon coherence may yield an upturn for periods similar to (and smaller than) a phonon mean free path.<sup>9,10</sup> However, the control over thermal conductivity in layered materials is not limited to simple size effects, as in particular for inorganic–organic materials, the drastic mismatch of the vibrational properties and the control over the bond strength over the internal interfaces may allow for further suppression of phonon transport.<sup>11,12</sup> Regarding inorganic–organic materials, the use of organic layers of appropriate thicknesses could also allow for the exploitation of phonon filtering realized due to interference effects within the organic layer.<sup>13</sup> In particular, a further degree of freedom to material design is brought about by the fact that the use of carbon in the fabrication of inorganic–organic interfaces is not limited to molecular organic layers, as interestingly also van-der-Waals bonded graphene interlayers have been demonstrated to have a lowering effect on thermal boundary conductance.<sup>14,15</sup>

An intriguing route for mixing inorganic materials and organic materials with highly dissimilar properties in a controlled manner is to employ atomic layer deposition (ALD) and molecular layer deposition (MLD) techniques in combination (ALD/MLD).<sup>16</sup> Besides simple homogeneous hybrid thin-film materials, such a combinatorial approach enables one to fabricate inorganic–organic superlattices with atomic/molecular monolayer precision *via* self-limiting surface reactions.<sup>17–19</sup> The self-limited film growth moreover allows for conformal coating of nanostructures, the key requirement for many future applications.<sup>20,21</sup> Recently, notably low thermal conductivity values were realized for ZnO-based ALD/MLD-fabricated hybrid structures obtained *via* incorporation of molecular organic layers; this observation has attracted great interest in thermal properties of ALD/MLD hybrid thin films – in particular for low-temperature thermal-barrier and thermoelectric applications.<sup>22,23</sup>

<sup>a</sup>Department of Chemistry, Aalto University, FI-00076 Aalto, Finland. E-mail: maarit.karppinen@aalto.fi

<sup>b</sup>Department of Mechanical and Aerospace Engineering, University of Virginia, Charlottesville, Virginia 22904, USA

Titanium dioxide is an n-type semiconductor generally known for its photocatalytic properties. However, the recent discovery of high electronic conductivity for heavily Nb-doped anatase thin films has directed increasing attention towards the transport properties – including thermoelectric properties – of  $\text{TiO}_2$ .<sup>24,25</sup> In this paper we demonstrate that ultra-low thermal conductivity values can be achieved in high-temperature-tolerant electronically conducting  $[(\text{TiO}_2)_m\text{C}_{k=1}]_n$  superlattice thin films by harnessing phonon-boundary scattering at the sub-nanometer-thick graphitic internal-interfaces, and that such interlayers can be formed from monomolecular-thick hydroquinone-based organic layers through a reductive annealing treatment of  $[(\text{TiO}_2)_m(\text{Ti}-\text{O}-\text{C}_6\text{H}_4-\text{O}-)_{k=1}]_n$  films grown using the ALD/MLD technique. Furthermore, we show that an incremental decrease in the thermal conductivity values is achieved by the addition of Nb point-defects into the  $\text{TiO}_2$  matrix.

## Experimental

We fabricated a series of  $\sim 100$  nm thick  $[(\text{TiO}_2)_m(\text{Ti}-\text{O}-\text{C}_6\text{H}_4-\text{O}-)_{k=1}]_n$  superlattice thin films on MgO and Si substrates at  $210^\circ\text{C}$  *via* the ALD/MLD route described in detail previously.<sup>19</sup> In brief, the fabrication route consisted of alternate chemisorption of the precursor vapors of  $\text{TiCl}_4$  (0.2 s),  $\text{H}_2\text{O}$  (0.1 s) and hydroquinone (HQ) (15 s) onto the substrate surface;  $\text{N}_2$  was used as the carrier gas to transport the precursor vapors into the ALD reactor (Picosun R100), and as a purging gas, that removes any unreacted precursor molecules after each precursor pulse. To deposit a superlattice with  $n$  periods, a set of  $m$  alternate pulses of  $\text{TiCl}_4$  and  $\text{H}_2\text{O}$  followed by one ( $k = 1$ ) cycle of the  $\text{TiCl}_4$  and HQ precursors were repeated  $n$  times. Niobium-substituted superlattice films with the composition of  $[(\text{Ti}_{0.75}\text{Nb}_{0.25}\text{O}_2)_m(\text{Ti}-\text{O}-\text{C}_6\text{H}_4-\text{O}-)_{k=1}]_n$  were fabricated by replacing every fourth  $\text{TiCl}_4$  pulse for the  $\text{TiO}_2$  block by a

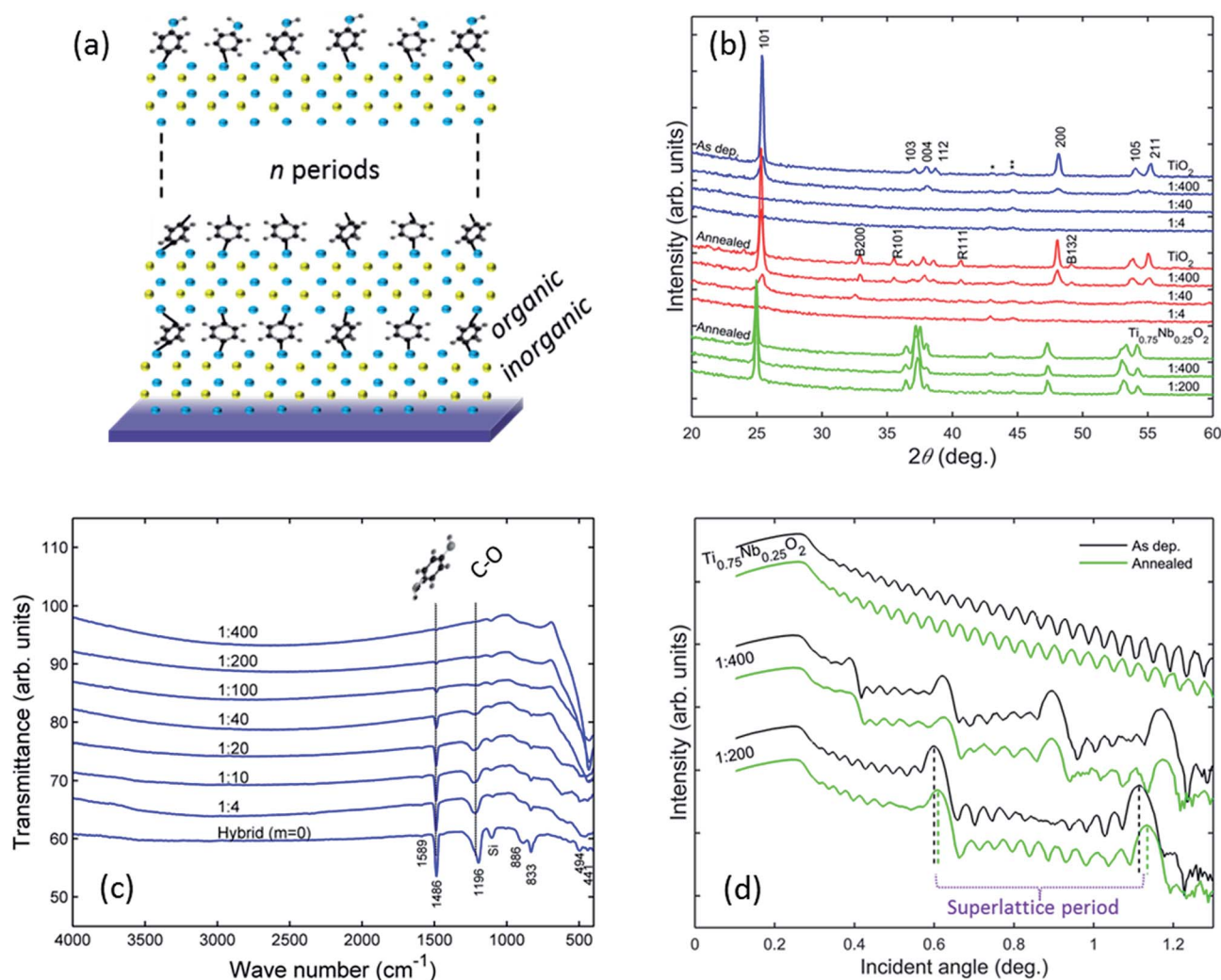


**Fig. 1** (a) An illustration of the  $[(\text{Ti}_{1-x}\text{Nb}_x\text{O}_2)_m(\text{Ti}-\text{O}-\text{C}_6\text{H}_4-\text{O}-)_{k=1}]_n$  superlattice structures with single layers of the  $(\text{Ti}-\text{O}-\text{C}_6\text{H}_4-\text{O}-)_{k=1}$  hybrid between octahedrally-coordinated  $\text{Ti}_{1-x}\text{Nb}_x\text{O}_2$  ( $x = 0$  or  $0.25$ ) layers. (b) GIXRD patterns for the superlattices with the main peaks indexed to the anatase structure of  $\text{TiO}_2$ , small impurities due to the rutile (R) and brookite (B) phases and the tiny modulations \* due to the MgO substrate and \*\* the substrate holder. (c) FTIR spectra for the films with  $x = 0$  and  $k : m$  in the range of  $1 : 400$ – $1 : 4$  and for the  $m = 0$  hybrid. (d) XRR patterns for the films with  $x = 0.25$  and  $k : m$  ratio of  $1 : 400$  and  $1 : 200$ , as well as for the purely inorganic  $\text{Ti}_{0.75}\text{Nb}_{0.25}\text{O}_2$  film. The GIXRD and XRR results are shown for both as-deposited films and for the films obtained *via* annealing in  $\text{Ar}/\text{H}_2$  gas at  $600^\circ\text{C}$ .

Nb(OEt)<sub>5</sub> (1 s) exposure.<sup>26</sup> An illustration of the targeted superlattice structures is shown in Fig. 1(a).

In order to determine the crystal structure of the thin films materials, a grazing incidence X-ray diffraction technique (GIXRD; PANalytical X'Pert Pro MPD diffractometer, Cu K<sub>α</sub>) was employed; for X-ray reflectivity (XRR) studies the same instrument was operated in the reflection mode, and the obtained XRR patterns provided us with information for the determination of the film thicknesses and for the verification of the superlattice structures, *i.e.*, that those well defined internal interface structures were indeed formed. Fourier transform infrared spectroscopy (FTIR; Nicolet magma 750 spectrometer) was utilized in the determination of the chemical state of the inorganic–organic films – in particular, to verify the incorporation of the organic component (HQ) into the film structure.

The as-deposited films with molecular HQ-based organic layers were subjected to strongly reductive post-deposition annealing – (Nabertherm GmbH RS 80/500/11) at 600 °C for 6 h in a tube furnace by flowing a 5% H<sub>2</sub>/Ar mixture (VARIGON® H5) as a reductive gas – in order to convert the molecular component into graphitic carbon. The carbon content of the annealed films was studied by means Raman spectroscopy (Thermo Fisher Scientific DXR-Raman microscope, 532 nm laser) and a subsequent fitting procedure was applied to the data, described more in detail in the Results and discussion section, to enable a more-in-depth discussion. The cross-plane thermal conductivity values were obtained *via* time-domain thermoreflectance (TDTR) – a technique that uses a combination of laser pulses to reveal the thermal properties of the sample: first, pump pulses introduce a stimulus of thermal energy to a metal transducer (here Al) on the sample surface, and second, probe pulses detect the consequent change in reflectance determined by the thermal properties of the sample.<sup>27–29</sup>

## Results and discussion

The as-deposited TiO<sub>2</sub> film crystallizes with the anatase structure as evidenced by GIXRD studies (Fig. 1(b)). However, the introduction of the organic layers suppresses the crystallinity of the superlattice films in a way that for  $k : m \leq 1 : 200$  the films are amorphous. The as-deposited Nb-substituted superlattice films are amorphous, as a consequence of the amorphous character of the Ti<sub>0.75</sub>Nb<sub>0.25</sub>O<sub>2</sub> matrix. The aromatic rings from the HQ precursor molecules are delivered to the structure intact as the FTIR spectra show a prominent absorption peak at around 1486 cm<sup>-1</sup> corresponding to the C=C stretching in the aromatic rings from the HQ precursor and a weak aromatic ring signal at 1589 cm<sup>-1</sup> (Fig. 1(c)). We also see a broad C–O stretching signal at around 1196 cm<sup>-1</sup> indicating that the molecular monolayers of the aromatic rings readily bond *via* oxygen atoms to the inorganic matrix. Furthermore, the XRR reflectograms show well-defined constructive interference patterns stemming from the molecular layers – a fact that confirms the formation of the targeted superlattice structures with single-molecular layers periodically sandwiched between the wider inorganic layers (Fig. 1(d)).

In an attempt to transform the molecular HQ-based organic layers in the as-deposited films into graphitic carbon layers, the films were subjected to strongly reductive post-deposition annealing; as a result the crystallinity of the films is notably enhanced such that even the [(TiO<sub>2</sub>)<sub>m</sub>(Ti–O–C<sub>6</sub>H<sub>4</sub>–O)<sub>k=1</sub>]<sub>n</sub> film with  $k : m$  of 1 : 40 yields moderate reflections. During the annealing step, minor impurities of the rutile and the brookite structures of TiO<sub>2</sub> form within the anatase matrix, which is prevented by Nb-substitution. Note that Nb indeed substitutes Ti in the structure, as the anatase peaks are seen to shift towards lower angles as a sign of an increase in unit cell volume (Fig. 1(b)). Given the high annealing temperature, it is remarkable that the annealing treatment retains the internal interfaces of the superlattice structure as is effectively verified from the XRR patterns shown in Fig. 1(d). The very small difference between the patterns for the as-deposited and the annealed films, *i.e.*, the fine widening of the fringes (compare the superlattice periods for the 1 : 200 sample marked with the dashed lines in Fig. 1(d)) can be ascribed to the increased film density and hence reduced film thickness due to both the improved crystallinity of the inorganic matrix and the probable contraction of the organic layers.

To get more insight into the carbon content in the fine internal interface layers of our annealed superlattice films, we studied the films by means of Raman spectroscopy. The results are shown in Fig. 2 in the wavenumber range of 1050–3000 cm<sup>-1</sup> for the Nb-doped films, denoted now as [(Ti<sub>0.75</sub>Nb<sub>0.25</sub>O<sub>2</sub>)<sub>m</sub>C<sub>k=1</sub>]<sub>n</sub>; the spectra show prominent peaks for sp<sup>2</sup> carbon at 1338 cm<sup>-1</sup> and 1602 cm<sup>-1</sup>, typically labeled as disordered D and graphitic G, respectively, and a modulated bump between 2400 and 3000 cm<sup>-1</sup> consisting of second-order peaks of D peak overtone G' and the combination mode D + G.<sup>30,31</sup> The D peak is a breathing mode of A<sub>1g</sub> symmetry with its intensity strictly connected to the presence of six-fold aromatic rings; the mode is

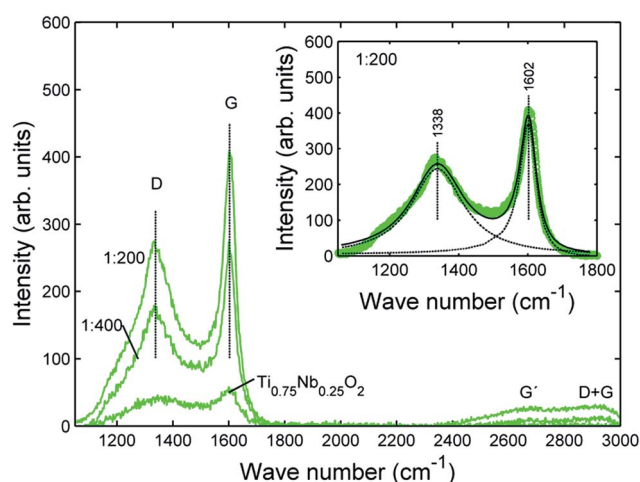


Fig. 2 Raman spectra of the [(Ti<sub>0.75</sub>Nb<sub>0.25</sub>O<sub>2</sub>)<sub>m</sub>C<sub>k=1</sub>]<sub>n</sub> superlattice thin films with the  $k : m$  ratios of 1 : 400 and 1 : 200, as well as for the purely inorganic Ti<sub>0.75</sub>Nb<sub>0.25</sub>O<sub>2</sub> film, obtained *via* annealing in Ar/H<sub>2</sub> gas at 600 °C. The inset shows fitting of the D and G peaks using a Lorentzian for the D peak and a Breit–Wigner–Fano distribution for the G peak.

forbidden in perfect graphite and only becomes active in the presence of disorder. The G peak stems from bond-stretching motion of pairs of carbon atoms both in rings and chains, and has  $E_{2g}$  symmetry. We fitted the spectral range of the D and G peaks using a Lorentzian for the D peak and a Breit–Wigner–Fano distribution for the G peak (inset of Fig. 2) in order to further evaluate the carbon content in our films. Based on the model of Ferrari and Robertson,<sup>30</sup> the maximally high G position of  $1602\text{ cm}^{-1}$  indicates the carbon layers in our films to have nanocrystalline nature. The ratio for integrated intensities yields  $A(D)/A(G) \approx 1.7$ , whereas for the comparison of the peak heights a value  $I(D)/I(G) \approx 0.7$  is obtained. Supposing that the comparison of the areas  $A(D)/A(G)$  gives appropriate information, the picture with nanocrystalline graphite is supported. However, as a sign of a degree of amorphousness and disorder, the D peak is found markedly broader in comparison to the G peak. As for amorphous carbon the information on the less distorted rings should be better reflected in the height of the D peak, rather than in its area,  $I(D)/I(G)$  comparison could be justified. According to ref. 30, the value  $I(D)/I(G) \approx 0.7$  should anyhow coexist with a notably lower G position value than  $1602\text{ cm}^{-1}$  – a consideration that leaves us with an ambiguity. In the end, in accordance with ref. 32, the carbon layers in our annealed superlattice thin films are probably best described as a mixture of nanocrystalline graphite and amorphous carbon, as crystallinity is seen in the high G position value and amorphous character in the broadening of the D peak.

The present inorganic–organic interfaces enable a marked suppression of heat transport in the present inorganic–organic superlattices, as was verified by means of the TDTR technique. In Fig. 3, we show the results for cross-plane thermal conductivities  $\kappa$  determined from the TDTR data for both the as-

deposited superlattice thin films with molecular aromatic carbon layers and the annealed superlattice films with graphitic carbon layers. The annealed  $\text{TiO}_2$  film has  $\kappa$  of  $6.78 \pm 0.40\text{ W m}^{-1}\text{ K}^{-1}$ , which is in good agreement with the literature value of  $\sim 6\text{ W m}^{-1}\text{ K}^{-1}$  for anatase  $\text{TiO}_2$  thin films.<sup>33</sup> In comparison to the purely inorganic  $\text{TiO}_2$  films, graphitic carbon layers in the  $[(\text{TiO}_2)_m\text{C}_{k=1}]_n$  superlattices markedly decrease the  $\kappa$  values down to  $3.79 \pm 0.30$ ,  $1.49 \pm 0.10$  and  $0.66 \pm 0.04\text{ W m}^{-1}\text{ K}^{-1}$  for  $k:m$  ratios of 1:400, 1:40 and 1:4, respectively; note that the overall decrease is as large as ten-fold and that the minimum lies greatly below the amorphous limit for  $\text{TiO}_2$  measured here as  $1.33 \pm 0.10\text{ W m}^{-1}\text{ K}^{-1}$ . For purely inorganic  $\text{TiO}_2$ , addition of Nb point-defects as phonon scattering centers reduces  $\kappa$  to  $3.49 \pm 0.30\text{ W m}^{-1}\text{ K}^{-1}$  for the  $\text{Ti}_{0.75}\text{Nb}_{0.25}\text{O}_2$  film. An incremental decrease of  $\kappa$  is seen for the  $[(\text{Ti}_{0.75}\text{Nb}_{0.25}\text{O}_2)_m\text{C}_{k=1}]_n$  superlattices *via* the introduction of the graphitic layers, as the  $\kappa$  value for the film with  $k:m$  of 1:400 is found to be as low as  $1.68 \pm 0.15\text{ W m}^{-1}\text{ K}^{-1}$ . The fact that the thermal conductivity values decrease with the decreasing superlattice period indicates that cross-plane thermal transport through the superlattices is predominately suppressed by incoherent boundary scattering of phonons.<sup>9,10</sup> This is valid as the heat transport here is indeed phonon dominated, as for the  $[(\text{TiO}_2)_m\text{C}_{k=1}]_n$  superlattices with electronic resistivity around  $1 \times 10^{-1}\text{ }\Omega\text{ m}$ , the Wiedemann–Franz law  $\kappa_e = L\rho^{-1}T$ , where  $L (=2.45 \times 10^{-8}\text{ W }\Omega\text{ K}^{-2})$  is the Lorentz number,  $\rho$  the electronic resistivity and  $T$  the temperature, yields negligible contribution for electrons of  $\kappa_e/\kappa \approx 7 \times 10^{-3}$  at room temperature. The thermal conductivity of the Nb-doped films is phonon dominated, though, electrons do contribute moderately: the resistivity values for the  $\text{Ti}_{0.75}\text{Nb}_{0.25}\text{O}_2$  and the respective  $k:m = 1:400$  superlattice were measured to be  $2.7 \times 10^{-3}\text{ }\Omega\text{ m}$  and  $1.2 \times 10^{-3}\text{ }\Omega\text{ m}$  that yield ratios  $\kappa_e/\kappa \approx 0.08$  and  $\kappa_e/\kappa \approx 0.36$ , hence confirming the fact that the reduction in thermal conductivity is due to the increased phonon scattering. Note that the present  $[(\text{Ti}_{1-x}\text{Nb}_x\text{O}_2)_m\text{C}_{k=1}]_n$  superlattice structures are stable at high temperatures of at least  $600\text{ }^\circ\text{C}$  – a fact that makes these structures particularly interesting for high-temperature applications.

The thermal conductivity values for the as-deposited superlattices show a similar decreasing trend with decreasing superlattice period to that observed for the annealed ones. Overall, the  $\kappa$  values for the  $[(\text{TiO}_2)_m(\text{Ti}-\text{O}-\text{C}_6\text{H}_4-\text{O})_{k=1}]_n$  films are slightly lower than those for the  $[(\text{TiO}_2)_m\text{C}_{k=1}]_n$  films, which can most likely be ascribed to improved crystallinity upon the annealing treatment, and indeed the lowest  $\kappa$  value among the present sample series, *i.e.*,  $0.62 \pm 0.04\text{ W m}^{-1}\text{ K}^{-1}$  is found for the as-deposited  $[(\text{TiO}_2)_m(\text{Ti}-\text{O}-\text{C}_6\text{H}_4-\text{O})_{k=1}]_n$  superlattice film with  $k:m$  of 1:4. The as-deposited films have very high electronic resistance and consequently electrons do not make an important contribution to the heat transport. The results for the as-deposited  $[(\text{TiO}_2)_m(\text{Ti}-\text{O}-\text{C}_6\text{H}_4-\text{O})_{k=1}]_n$  films confirm the efficient suppression of thermal conductivity we reported previously for ZnO analogues of the present superlattices, and is in line with the results for the Zn-based hybrid from DEZ and HQ or ethylene glycol precursors of the type,  $k:m = 1:1$  or  $m = 0$ , with the present notation.<sup>22,23</sup> Note that, the present results demonstrate that in the ALD/MLD superlattices thermal

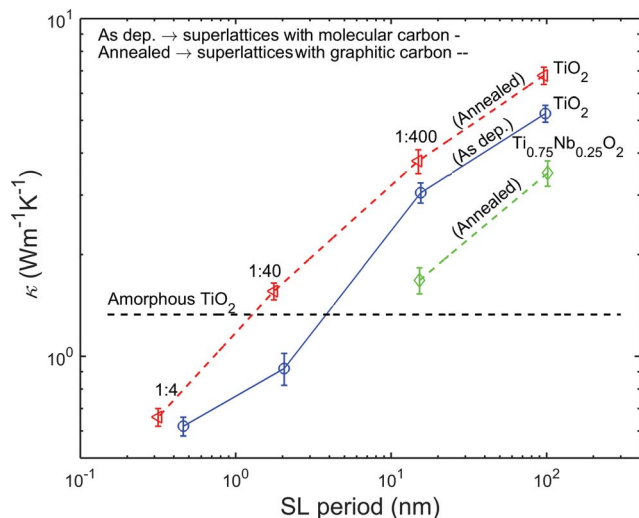


Fig. 3 Thermal conductivity values plotted against the superlattice period for the as deposited  $[(\text{TiO}_2)_m(\text{Ti}-\text{O}-\text{C}_6\text{H}_4-\text{O})_{k=1}]_n$  films with the  $k:m$  ratio of 1:400, 1:40 and 1:4 (in blue) and the same films after annealing in  $\text{Ar}/\text{H}_2$  gas at  $600\text{ }^\circ\text{C}$  (in red), and also for the annealed  $[(\text{Ti}_{0.75}\text{Nb}_{0.25}\text{O}_2)_m\text{C}_{k=1}]_n$  films with  $k:m = 1:400$  (in green). Note that in each case the value at the superlattice period of  $10^2\text{ nm}$  is for the corresponding purely inorganic film with  $k = 0$ .

conductivity can be systematically controlled by the superlattice period hence complementing the results of ref. 22 and 23. Our recent results for the ZnO-based superlattices indicated that the phonon transmission through the molecular monolayers (from HQ) is actually hardly affected by the vibrational properties of the aromatic rings and that the suppression in thermal conductivity values is mainly due to the reduction in the ZnO layer thickness, *i.e.*, the superlattice period.<sup>34</sup> This is consistent with the reduction in thermal conductivities for the present TiO<sub>2</sub>-based superlattices. Regarding the possibilities to further suppress the thermal conductivity values obtained here, interesting questions arise, *e.g.*, the role of the organic layer thickness.

## Conclusions

The cross-plane thermal conductivity in inorganic–organic TiO<sub>2</sub>:C superlattices can be progressively hindered by decreasing the superlattice period – an effect that is mediated by incoherent boundary scattering at the sub-nanometer-thick graphitic layers within the TiO<sub>2</sub> matrix. In the present superlattices, we see a ten-fold decrease down to an ultra-low value of  $\sim 0.66 \text{ W m}^{-1} \text{ K}^{-1}$  – notably below the amorphous limit – for a superlattice period of  $\sim 0.3 \text{ nm}$ . The TiO<sub>2</sub>:C superlattices can be fabricated at first periodically confining molecular hydroquinone-based monolayers between thicker TiO<sub>2</sub> layer blocks by means of a self-limiting ALD/MLD technique, and then subsequently transforming the molecular layers into very thin graphitic layers *via* reductive annealing treatment. It is of note that, by using such a fabrication route, the number and the spacing of the thin graphitic layers are perfectly computer controlled and no transfer techniques are needed. Also note that, the present fabrication route is not limited to the TiO<sub>2</sub>-organic material pair but is applicable to a wide library of materials that can be combined *via* the ALD/MLD chemistries to conformally coat a variety of three-dimensional nanostructures for future applications. Furthermore, tolerance to the employed high-temperature fabrication conditions indicates notable temperature stability for the present-kind superlattices and makes the structures attractive for high-temperature thermal barriers and thermoelectric applications.

## Acknowledgements

The present work has received funding from the European Research Council under the European Union's Seventh Framework Programme (FP/2007–2013)/ERC Advanced Grant Agreement (no. 339478) as well as the Aalto Energy Efficiency Research Programme and the U.S. Army Research Office (W911NF-13-1-0378).

## Notes and references

- W. S. Capinski and H. J. Maris, *Phys. B*, 1996, **219** & **220**, 699–701.
- G. Chen, *Phys. Rev. B: Condens. Matter Mater. Phys.*, 1998, **57**(23), 14958–14973.
- T. Yao, *Appl. Phys. Lett.*, 1987, **51**, 1798–1800.
- G. Chen, *J. Heat Transfer*, 1997, **119**(2), 220–229.
- R. M. Costescu, D. G. Cahill, F. H. Fabreguette, Z. A. Sechrist and S. M. George, *Science*, 2004, **303**, 989–990.
- C. Chiritescu, D. G. Cahill, N. Nguyen, D. Johnson, A. Bodapati, P. Keblinski and P. Zschack, *Science*, 2007, **315**, 351–353.
- K. E. Goodson, *Science*, 2007, **315**, 342–343.
- P. M. Norris, N. Q. Le and C. H. Baker, *J. Heat Transfer*, 2013, **135**, 061604.
- M. V. Simkin and G. D. Mahan, *Phys. Rev. Lett.*, 2000, **84**(5), 927–930.
- J. Ravichandran, A. K. Yadav, R. Cheaito, P. B. Rossen, A. Soukiassian, S. J. Suresha, J. C. Duda, B. M. Foley, C.-H. Lee, Y. Zhu, A. W. Lichtenberger, J. E. Moore, D. A. Muller, D. G. Schlom, P. E. Hopkins, A. Majumdar, R. Ramesh and M. A. Zurbuchen, *Nat. Mater.*, 2014, **13**, 168–172.
- R. Y. Wang, R. A. Segalman and A. Majumdar, *Appl. Phys. Lett.*, 2006, **89**, 173113.
- P. J. O'Brien, S. Shenogin, J. Liu, P. K. Chow, D. Laurencin, P. H. Mutin, M. Yamaguchi, P. Keblinski and G. Ramanath, *Nat. Mater.*, 2013, **12**, 118–122.
- L. Hu, L. Zhang, M. Hu, J.-S. Wang, B. Li and P. Keblinski, *Phys. Rev. B: Condens. Matter Mater. Phys.*, 2010, **81**, 235427.
- W.-P. Hsieh, A. S. Lyons, E. Pop, P. Keblinski and G. D. Cahill, *Phys. Rev. B: Condens. Matter Mater. Phys.*, 2011, **84**, 184107.
- P. E. Hopkins, M. Baraket, E. V. Barnat, T. E. Beechem, S. P. Kearney, J. C. Duda, J. T. Robinson and S. G. Walton, *Nano Lett.*, 2012, **12**, 590–595.
- P. Sundberg and M. Karppinen, *Beilstein J. Nanotechnol.*, 2014, **5**, 1104–1136.
- K.-H. Yoon, K.-S. Han and M.-M. Sun, *Nanoscale Res. Lett.*, 2012, **7**, 71.
- T. Tynell, I. Terasaki, H. Yamauchi and M. Karppinen, *J. Mater. Chem. A*, 2013, **1**, 13619–13624.
- J.-P. Niemelä and M. Karppinen, *Dalton Trans.*, 2015, **44**, 591–597.
- M. Knez, K. Nielsch and L. Niinistö, *Adv. Mater.*, 2007, **19**, 3425–3438.
- J. Malm, E. Sahrmo, M. Karppinen and R. H. A. Ras, *Chem. Mater.*, 2010, **22**, 3349–3352.
- J. Liu, B. Yoon, E. Kuhlmann, M. Tian, J. Zhu, S. M. George, Y.-C. Lee and R. Yang, *Nano Lett.*, 2013, **13**, 5594–5599.
- T. Tynell, A. Giri, J. Gaskins, P. E. Hopkins, P. Mele, K. Miyazaki and M. Karppinen, *J. Mater. Chem. A*, 2014, **2**, 12150–12152.
- Y. Furubayashi, T. Hitosugi, Y. Yamamoto, K. Inaba, G. Kinoda, Y. Hirose, T. Shimada and T. Hasegawa, *Appl. Phys. Lett.*, 2005, **86**, 252101.
- J. Jaćimović, R. Gaál, A. Magrez, J. Piatek, L. Porró, S. Nakao, Y. Hirose and T. Hasegawa, *Appl. Phys. Lett.*, 2013, **102**, 013901.
- J.-P. Niemelä, Y. Hirose, T. Hasegawa and M. Karppinen, *Appl. Phys. Lett.*, 2015, **106**, 042101.
- D. G. Cahill, *Rev. Sci. Instrum.*, 2004, **75**(12), 5119–5122.

- 28 A. J. Schmidt, X. Chen and G. Chen, *Rev. Sci. Instrum.*, 2008, **79**, 114902.
- 29 P. E. Hopkins, J. R. Serrano, L. M. Phinney, S. P. Kearney, T. W. Grasser and C. T. Harris, *J. Heat Transfer*, 2010, **132**, 081302.
- 30 A. C. Ferrari and J. Robertson, *Phys. Rev. B: Condens. Matter Mater. Phys.*, 2000, **61**(20), 14095–14107.
- 31 M. A. Pimenta, G. Dresselhaus, M. S. Dresselhaus, L. G. Cançado, A. Jorio and R. Saito, *Phys. Chem. Chem. Phys.*, 2007, **9**, 1276–1291.
- 32 A. I. Abdulagatov, K. E. Terauds, J. J. Travis, A. S. Cavanagh, R. Raj and S. M. George, *J. Phys. Chem. C*, 2013, **117**, 17442–17450.
- 33 C. Tasaki, N. Oka, T. Yagi, N. Taketoshi, T. Baba, T. Kamiyama, S. Nakamura and Y. Shigesato, *Jpn. J. Appl. Phys.*, 2012, **51**, 035802.
- 34 A. Giri, T. Tynell, J.-P. Niemelä, J. Gaskins, B. F. Donovan, M. Karppinen and P. E. Hopkins, *Phys. Rev. Lett.*, 2015, under review.